This article has been accepted for publication in a future issue of this journal, but has not been fully edited. Content may change prior to final publication. Citation information: DOI 10.1109/LAWP.2019.2924727, IEEE Antennas and Wireless Propagation Letters

Increasing Efficiency of Leaky-Wave Antenna by Using Substrate Integrated Slab Waveguide

Enrico Massoni, *Graduate Student Member, IEEE*, Maurizio Bozzi, *Fellow, IEEE*, and Ke Wu, *Fellow*, *IEEE*

***Abstract*—This letter presents a possibility of increasing the radiation efficiency of double-sided leaky-wave antennas (LWAs) by using the substrate integrated slab waveguide (SISW). The idea originates from the fact that double-sided LWAs usually operate on the second mode, and the attenuation constant of the second mode in the SISW is smaller than that in the standard SIW. This inherently leads to an increase of antenna radiation efficiency, as less power is dissipated by the traveling wave. In order to prove this concept, two antennas have been designed with the same characteristics (central frequency of 28 GHz, pointing angle of 50°, and beamwidth of 10°), one based on SIW and the other based on SISW. Our experimental verification yields 64% radiation efficiency for the SIW LWA and 80% radiation efficiency for the SISW LWA, thus proving the theoretical and simulated predictions.**

***Index Terms*—Antenna radiation efficiency, leaky-wave antenna (LWA), substrate integrated waveguide (SIW), substrate integrated slab waveguide (SISW).**

I. INTRODUCTION

THE DEVELOPMENT of future communication systems and the advent of the fifth generation of mobile communication (5G) require the introduction of new classes of high performance antennas [1]. In particular, these applications are expected to demand for high data rate and to cope with massive traffic volume [2]. Moreover, the frequency spectrum identified to provide those services is located in the millimeter-wave range, with the first applications centered at 28 GHz [3].

These high-frequency systems require simple, compact, low-cost, low-profile, and high directivity antennas, and therefore a natural candidate that presents those features is the planar leaky-wave antenna (LWA). Furthermore, these antennas exhibit high gain and easy integration with other planar structures.

For all these reasons, a large-scaled investigation in the recent years has led to the development of planar LWAs with different types of transmission lines [4]-[6]. Among them, the substrate integrated waveguide (SIW) technology [Fig. 1(*a*)] is attracting much interest of researchers thanks to its moderately low losses, simplicity, and cost-effectiveness [7].

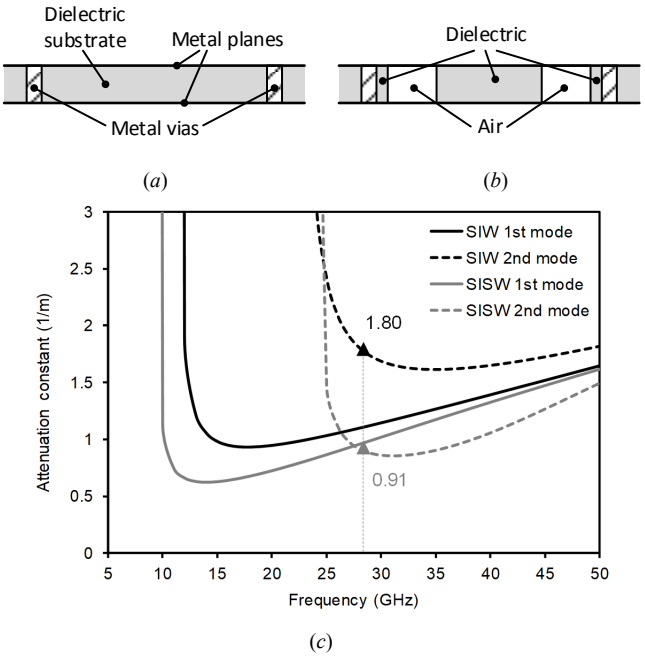

Fig. 1. Comparison between SIW and the SISW: (*a*) Geometry of SIW; (*b*) Geometry of SISW; (*c*) attenuation constants for the two lines (first and second modes).

Various SIW LWA prototypes have been proposed [8]-[9]. In particular, a double-sided SIW LWA with increased directivity in the *E*-plane was proposed in [10]-[11], that operates on the second (TE_{20}) SIW mode and allows for a full control of the complex propagation constant.

Furthermore, in a recent work [12], it was observed that the attenuation constant of the second mode of a substrate integrated slab waveguide (SISW) [13] [Fig. 1(*b*)] is significantly lower than the attenuation constant of the second mode of the corresponding SIW realized on the same substrate. This feature is exploited in this letter to increase the radiation efficiency of double-sided planar LWAs. In fact, a lower attenuation constant of the transmission line leads to a smaller amount of loss of the traveling wave. Therefore, by replacing the main SIW transmission line with an SISW, it is possible to implement an SISW LWA with similar radiation characteristics but higher efficiency.

This letter is organized as follows. An investigation of the attenuation constant in SIW and SISW transmission lines is presented in Sec. II. Subsequently, the design of an SIW LWA and its prototype are presented in Sec. III. Afterwards, in Sec. IV, an SISW LWA with the practically identical radiation

Manuscript submitted May 5, 2019; revised June 15, 2019, accepted June 19, 2019. This work has been partially supported by the Associazione Italiana di Elettrotecnica, Elettronica, Automazione, Informatica, e Telecomunicazioni (AEIT) under the scholarship "Isabella Sassi Bonadonna".

E. Massoni was with the Department of Electrical, Computer and Biomedical Engineering, University of Pavia, 27100 Pavia, Italy. He is now with STMicroelectronics, R&D Department, AMS Group, 20864 Agrate Brianza, Italy (e-mail: enrico.massoni@st.com)

M. Bozzi is with the Department of Electrical, Computer and Biomedical Engineering, University of Pavia, 27100 Pavia, Italy (e-mail: maurizio.bozzi@unipv.it).

K. Wu is with the Department of Electrical Engineering, Poly-Grames Research Center, Polytechnique Montréal, Montréal, QC H3T-1J4, Canada (e-mail: ke.wu@polymtl.ca).

This article has been accepted for publication in a future issue of this journal, but has not been fully edited. Content may change prior to final publication. Citation information: DOI 10.1109/LAWP.2019.2924727, IEEE Antennas and Wireless Propagation Letters

characteristics as the previous SIW antenna is investigated, fabricated, and tested, to show the increased radiaton efficiency.

II. SISW VERSUS SIW

This section summarizes the properties of an SISW structure [13], [14] and compares them with those of the standard SIW [7]. While the SISW is commonly used to increase the single-mode bandwidth, it also exhibits lower attenuation constant of the second (quasi TE_{20}) mode [12]. This is possible thanks to the pattern of the TE_{20} mode, which exhibits a more intense electric field in the lateral air-filled portions of the SISW substrate. Consequently, the attenuation constant of the second mode in a properly designed SISW is generally smaller than the counterpart in the SIW implemented on the same dielectric substrate.

To quantitatively evaluate this phenomenon, the attenuation constants for the first and second modes of both SIW and SISW structures have been computed through the commercial electromagnetic solver ANSYS HFSS. Results are reported in Fig. 1(*c*). In this case, the substrate adopted is the RT/duroid® 6002 laminate ($\varepsilon_r=2.94$, $tg\delta=0.0012$, and thickness $h=0.508$ mm). The difference between the attenuation constant of the first mode of the SIW and of the SISW is not remarkable, as in both structures the electric field is mainly concentrated in the dielectric region. Conversely, a large difference is observed for the second mode. In particular, at the frequency of 28 GHz, the attenuation constant in the SISW is a half of the attenuation constant in the SIW.

Table I reports the comparison between the attenuation constants of the second mode of SIW and SISW, with two different dielectric substrates. The high performance RT/duroid® 6002 laminate is compared to the FR-4, a low-cost laminate. While the values of the attenuation constant are very different in the two substrates, due to the large difference in loss tangent of the dielectric materials, both examples show that the attenuation constant of the TE_{20} mode of SISW is significantly smaller than the one of SIW.

III. SIW LEAKY WAVE ANTENNA

The design of a double-sided SIW LWA is presented in this section, along the lines of [11]. A three-dimensional view of the structure is shown in Fig. 2. The antenna operates on the TE_{20} mode of SIW, as this allows an increased directivity in the *E* plane. In addition, it is possible to fully control the complex propagation constant by modifying the separation *P* between posts, responsible for the leakage rate, and the width *w* of SIW, responsible for the radiation pointing angle, as observed in [11].

TABLE I – COMPARISON OF ATTENUATION CONSTANTS EVALUATED AT 28 GHZ FOR DIFFERENT SUBSTRATES CHOICE

Material	ε_r	tgδ	Attenuation TE_{20} SIW [1/m]	Attenuation TE_{20} SISW [1/m]
FR-4	4.4	0.02	24.40	13.47
RT/duroid® 6002	2.94	0.0012	1.80	0.91

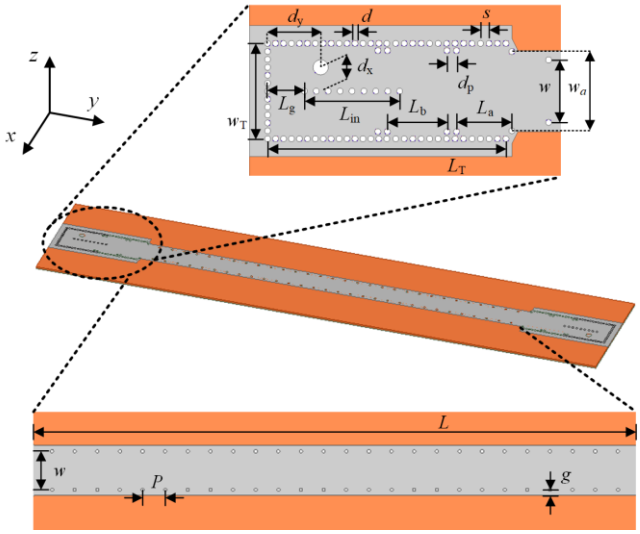

Fig. 2. Geometry of the SIW LWA (dimensions in mm: $w_T=8$, $d_y=4.45$, $d_x=w_T/4=2$, $L_g=3.08$, $L_{in}=8$, $L_a=4.65$, $L_b=5$, $L_T=20$, $w_a=6.65$, $d_p=1$, $s=1$, $d=0.5$, $w=5.25$, $P=3.08$, $g=0.78$, $L=95.5$).

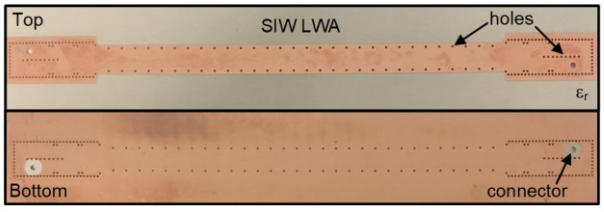

Fig. 3. Photograph of the SIW LWA prototype.

With regards to the design specifications, the operation frequency was selected $f=28$ GHz, the radiating pointing angle $\theta_{RAD}=50°$, and the beamwidth $\theta=10°$. Adopting the formula presented in [11], the total length of the LWA can be obtained. Subsequently, *w* and *P* are chosen to implement the desired values of α and β, as described in [10]–[11] and [15]. Finally, the extra metal gap is tuned, as in [11], to complete the design. In addition, for measurement purposes, a coaxial-to-SIW transition was adopted. The adopted transition excites the TE_{20} mode inside the structure and at the same time suppresses the propagation of the TE_{10} mode (Fig. 2). The solution is similar to the one adopted in [11].

A prototype of the SIW LWA is shown in Fig. 3. It is based on the RT/duroid® 6002 laminate (with $\varepsilon_r=2.94$, $tg\delta=0.0012$, and thickness $h=0.508$ mm). A laser machine was adopted to pattern the metal layers and to drill the holes, and subsequently the holes were metalized by electroplating. Finally, the connectors were inserted through the substrate and soldered both at the bottom and top metal plates.

The prototype was tested to validate the theoretical and simulated predictions. Fig. 4(*a*) shows the simulated (solid line) and measured (dashed line) normalized radiation pattern of the SIW LWA in the *H*-plane at 28 GHz. The measurements validate both the pointing angle of 50° and the beamwidth of 10°, thus demonstrating a good control of the complex propagation constant, as foreseen in the simulations. Moreover, the normalized radiation patterns in the *E*-plane are reported in Fig. 4(*b*). In this case, the *E*-plane is defined along

This article has been accepted for publication in a future issue of this journal, but has not been fully edited. Content may change prior to final publication. Citation information: DOI 10.1109/LAWP.2019.2924727, IEEE Antennas and Wireless Propagation Letters

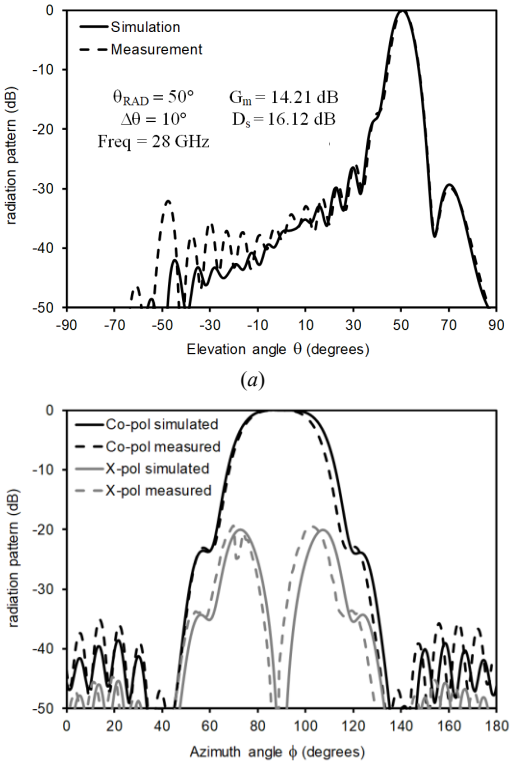

Fig. 4. Measured and simulated normalized radiation pattern of the SIW LWA, evaluated at the frequency f=28 GHz; (*a*) *H*-plane; (*b*) *E*-plane.

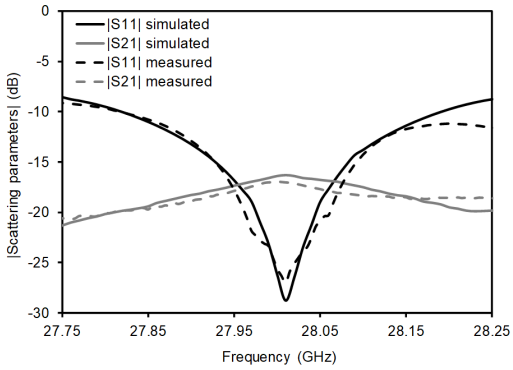

Fig. 5. Measured and simulated scattering parameters for the SIW LWA.

the angle of maximum radiation ($\theta_{RAD} = 50°$) and the angle ϕ assumes values in the span from 0° to 180°. Also in this case, measurement outcomes are in a good agreement with the simulated ones. Moreover, the cross-polarizaton is maintained quite low, both in simulation and measurement, more than 20 dB below the co-polarization level. Furthermore the co-polarization component has a -3 dB beamwidth of $\Delta\theta = 34°$ insimulation and $\Delta\theta = 30°$ in measurement, and the maximum gain is 14.36 dB in simulation and 14.21 dB in measurement. The radiation efficiency of the SIW LWA, computed as the ratio between measured gain and simulated directivity, is 64.4%. Finally, the scattering parameters versus frequency are reported in Fig. 5, showing a good input matching at 28 GHz as well as a very low transmission to the output port.

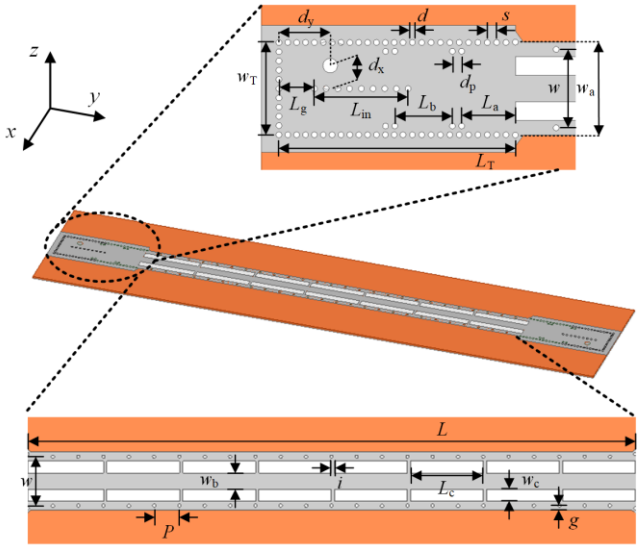

Fig. 6. Geometry of the SISW LWA (dimensions in mm: $w_T = 8$, $d_y = 4.45$, $d_x = w_T/4 = 2$, $L_g = 3.08$, $L_{in} = 8$, $L_a = 4.65$, $L_b = 5$, $L_T = 20.5$, $w = 6.8$, $w_a = 8$, $d_p = 1$, $s = 1$, $d = 0.5$, $w_b = 2.27$, $w_c = 1.7$, $P = 3.54$, $g = 0.6$, $L = 95.5$, $i = 0.508$, $L_c = 13.135$).

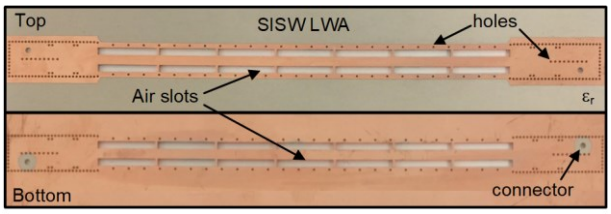

Fig. 7. Photograph of the SISW LWA prototype, prior to the application of the copper adhesive tape.

IV. SISW LEAKY WAVE ANTENNA

The design of a double-sided SISW LWA is discussed in this Section, with radiation characteristics identical to the SIW LWA, following the design rules presented in [11]. A 3D view of the antenna is shown in Fig. 6. Compared to the antenna proposed in Sec. III, this structure consists of a slight yet fundamental modification of the central transmission line that implements the antenna itself. The SIW-line is replaced by an SISW-line, with the central dielectric part and lateral air-filled portions. For mechanical considerations and manufacturing requirements, the central dielectric part has been connected to the lateral sides by means of small dielectric stubs. This solution presents a negligible effect in terms of transmission properties and has been taken into account in the simulation. The feeding is similar to the one adopted for the SIW LWA.

A prototype has been manufactured, with the same RT/duroid® 6002 laminate adopted for the SIW-LWA. Subsequently, a commercial adhesive copper tape (assumed with same conductivity of the copper, $\sigma = 5.8 \cdot 10^7$ S/m, as reported in the data sheet) was cut through a numerically controlled milling machine and subsequently attached both on the top and bottom planes, in order to close the structure. A picture of the prototype is shown in Fig. 7, prior to the application of the copper adhesive tape used to implement the

This article has been accepted for publication in a future issue of this journal, but has not been fully edited. Content may change prior to final publication. Citation information: DOI 10.1109/LAWP.2019.2924727, IEEE Antennas and Wireless Propagation Letters

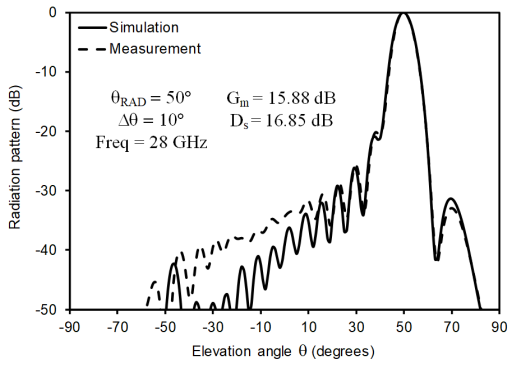

(*a*)

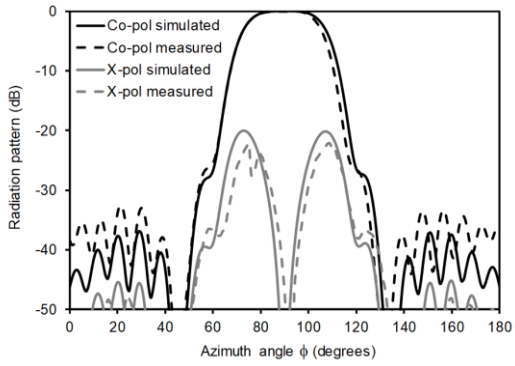

(*b*)

Fig. 8. Measured and simulated normalized radiation pattern of the SISW LWA, evaluated at the frequency f=28 GHz; (*a*) *H*-plane; (*b*) *E*-plane.

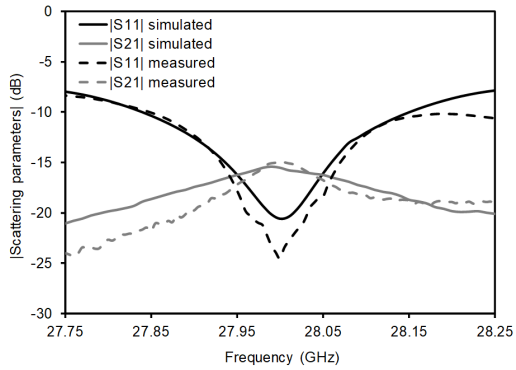

Fig. 9. Measured and simulated scattering parameters for the SISW LWA.

top and bottom metal planes, and prior to the soldering of the connectors.

The prototype has been tested to validate the theoretical and simulated predictions. Fig. 8(a) shows the simulated (solid line) and measured (dashed line) normalized radiation pattern of the SISW LWA in the H-plane at 28 GHz. The measurements validate both the pointing angle of 50° and the beamwidth of 10°, thus demonstrating a good control of the complex propagation constant, as foreseen in the simulations. Moreover, the normalized radiation patterns for the *E*-plane are also presented in Fig. 8(*b*). Also in this case, the *E*-plane is defined along the angle of maximum radiation ($\theta_{\mathrm{RAD}} = 50°$) and the angle ϕ assumes values in the span from 0° to 180°. In both cases, measured outcomes are in a good agreement with the simulated ones.

Moreover, the cross-polarization level is better than -20 dB in the simulation and -22 dB in the measurement, as depicted in Fig. 8(*b*). It has been observed that the co-pol component has a -3 dB beamwidth of $\Delta\theta$=34° in the simulation and $\Delta\theta$=32° in the measurement, and a maximum gain of 15.94 dB in the simulation and 15.88 dB in the measurement, leading to a radiation efficiency of 80.0% for the SISW LWA. The scattering parameters versus frequency are reported in Fig. 9.

To summarize, Table II highlights the radiation efficiency comparison between the two antennas analyzed in this work. At 28 GHz, the SIW LWA radiation efficiency is 64.4%, whereas the SISW LWA exhibits a higher radiation efficiency of 80.0%, thus validating the assumptions of the previous Sections.

TABLE II – RADIATION EFFICIENCY COMPARISON

Antenna	Measured gain (dB)	Simulated directivity (dB)	Radiation efficiency (%)
SIW LWA	14.21	16.12	64.4
SISW LWA	15.88	16.85	80.0

V. CONCLUSION

This letter presented a technique to increase the radiation efficiency of double-sided leaky-wave antennas (LWAs) by adopting the substrate integrated slab waveguide (SISW) technology. In fact, by choosing the SISW technology, it is possible to halve the attenuation constant of the second mode, when compared to the standard SIW solution, thus inherently leading to the overall increase of antenna radiation efficiency. To prove this concept, two prototypes with identical characteristics have been designed, manufactured and experimentally validated. The SIW LWA provided a measured maximum gain of 14.21 dB, resulting in a radiation efficiency of 64.4%. Conversely, the SISW LWA exhibited a measured maximum gain of 15.88 dB, correspondint to a radiation efficiency of 80.0%. The proposed structure represents an improved solution as a novel class of high radiation efficiency antennas for the novel fifth generation (5G) of mobile communication and for wireless sensors networks.

ACKNOWLEDGMENT

The authors would like to thank all the technicians of the Poly-Grames Research Center, Montréal, QC, Canada, for their valuable support and precious advice.

REFERENCES

[1] A. Osseiran, J. F. Monserrat, and P. Marsch, *5G Mobile and Wireless Communications Technology*. New York, NY, USA: Cambridge University Press, 2016.

[2] E. Dahlman, S. Parkvall, D. Astély, and H. Tullberg, "Advanced antenna solutions for 5G wireless access," *Proc. Asilomar ACSSC*, Nov. 2014, pp. 810-814.

[3] T. S. Rappaport *et al.*, "Millimeter wave mobile communications for 5G cellular: It will work!" *IEEE Access*, vol. 1, pp. 335-349, May 2013.

[4] A. A. Oliner and D. R. Jackson, "Leaky-wave antennas," in *Antenna Engineering Handbook*, 4th ed., J. L. Volakis, Ed. New York: McGraw-Hill, Jun. 2007, ch. 11.

[5] H. A. Diawuo and Y. B. Jung, "Broadband Proximity-Coupled Microstrip Planar Antenna Array for 5G Cellular Applications," *IEEE Antennas and Wireless Propagation Letters*, vol. 17, no. 7, pp. 1286-1290, July 2018.

[6] S. Alkaraki *et al*., "Compact and Low Cost 3D-Printed Antennas Metalized using Spray-Coating Technology for 5G mm-Wave Communication Systems," *IEEE Antennas and Wireless Propagation Letters*, vol. 17, no. 11, pp. 2051-2055, Nov. 2018.

[7] M. Bozzi, A. Georgiadis, and K. Wu, "Review of substrate integrated waveguide (SIW) circuits and antennas," *IET Microw. Antennas Propag.*, vol. 5, no. 8, pp. 909-920, June 2011.

[8] F. M. Monavar, S. Shamsinejad, R. Mirzavand, J. Melzer and P. Mousavi, "Beam-Steering SIW Leaky-Wave Subarray With Flat-Topped Footprint for 5G Applications," *IEEE Transactions on Antennas and Propagation*, vol. 65, no. 3, pp. 1108-1120, Mar. 2017.

[9] K. M. Mak, K. K. So, H. W. Lai and K. M. Luk, "A Magnetoelectric Dipole Leaky-Wave Antenna for Millimeter-Wave Application," *IEEE Transactions on Antennas and Propagation*, vol. 65, no. 12, pp. 6395-6402, Dec. 2017.

[10] A. J. Martinez-Ros, J. L. Gomez-Tornero and G. Goussetis, "Planar Leaky-Wave Antenna with Flexible Control of the Complex Propagation Constant," *IEEE Transactions on Antennas and Propagation*, vol. 60, no. 3, pp. 1625-1630, March 2012.

[11] A. J. Martinez-Ros, M. Bozzi and M. Pasian, "Double-Sided SIW Leaky-Wave Antenna with Increased Directivity in the E -Plane," *IEEE Transactions on Antennas and Propagation*, vol. 66, no. 6, pp. 3130-3135, June 2018.

[12] E. Massoni *et al*., "3-D Printed Substrate Integrated Slab Waveguide for Single-Mode Bandwidth Enhancement," *IEEE Microwave and Wireless Components Letters*, vol. 27, no. 6, pp. 536-538, June 2017.

[13] M. Bozzi *et al*., "Efficient analysis and experimental verification of substrate integrated slab waveguides for wideband microwave applications," *Int. J. RF Microw. Comput.-Aided Eng*., vol. 15, no. 3, pp. 296-306, May 2005.

[14] N.-H. Nguyen, A. Ghiotto, T.-P. Vuong, A. Vilcot, F. Parment, and K. Wu, "Slab Air-Filled Substrate Integrated Waveguide," *2018 IEEE MTT-S International Microwave Symposium (IMS2018)*, Philadelphia, PA, USA, June 10-15, 2018.

[15] M. Pasian, M. Bozzi and L. Perregrini, "A Formula for Radiation Loss in Substrate Integrated Waveguide," *IEEE Transactions on Microwave Theory and Techniques*, vol. 62, no. 10, pp. 2205-2213, Oct. 2014.